Inertial Focusing of Particles in Curved Microchannels

26 April 2021

Anna Kaehr (Honors Capstone), Emma Purcell, Kaylee Smith, Abigail Radomski, Sunitha Nagrath

Department of Chemical Engineering, University of Michigan, Ann Arbor, MI

Abstract

Inertial focusing is the migration of particles in flow laterally across a channel into well-defined equilibrium positions. In microfluidic channels, inertial focusing takes advantage of hydrodynamic interactions even at high flow speeds. Particle isolation through inertial focusing is a high throughput method of processing biological samples for point-of-care diagnostics. While photos provide qualitative analyses of inertial focusing, we desired quantitative characterization of these systems. In this study, we ran flow experiments, first with fluorescent polystyrene beads and later with cells in solution, through curved microchannels at controlled rates using a syringe pump. Our results from polystyrene bead experiments confirmed previous studies on flow through curved microchannels, in which particles are focused along both sides of the channel at low flow rates and transition towards the center of the channel as the flow rate increases. FWHM analysis also showed that the streamline width is minimized at an intermediate flow rate, indicating inertial focusing is optimized under that condition. As this method of analysis was confirmed with polystyrene beads, we further used this analysis method to characterize the focusing of cells in solution. To maximize both throughput and purity, microfluidic devices must be designed to operate at the highest flow rate at which effective separation from bulk fluid can occur. The device presented in this report indeed isolates the desired target cells to be studied in downstream characterization.

Introduction

Microfluidics is a technology that allows for efficient analyses of rare cell types that have been known to play a role in human disease such as cancer. To maximize both throughput and purity, microfluidic devices must be designed to operate at the highest capacity at which effective separation of target species from bulk fluid can occur.

Particle isolation through inertial focusing is a particularly high throughput and cost-effective method of processing biological samples for point-of-care diagnostics.[2] Inertial focusing is a technique in microfluidics that relies solely on hydrodynamics to control the motion of particles in confined channels. Due to the inertia and viscosity of the fluid, particles in flow migrate laterally across a channel into well-defined equilibrium positions.[1] Particle focusing is affected by microfluidic device design such as channel size and curvature, as well as by particle and fluid features such as size, density, and viscosity.

Inertial microfluidic devices are designed to run in the laminar flow regime, in which the ratio of inertial forces (a function of density, flow rate, and channel length) to viscous forces (a function of viscosity) is small. In this flow regime, the wall force pushes particles away from the device walls while the shear-induced lift force pushes particles back towards the device walls, resulting in a parabolic velocity profile. Focusing is highly depended on this parabolic velocity profile caused by competing forces within the channel flow. Additionally, device curvature influences a secondary type of flow called Dean flow, which is driven by centrifugal forces from the velocity differences at different points along the channel.

This report focuses on the study of inertial focusing of particles in curved microchannels. First presented in this report are the focusing results of polystyrene beads, which are simple homogenous particles. Then these results are compared with that of cells, which are highly heterogenous.

Methods

Device Fabrication

Soft lithography was used to cure polydimethylsiloxane (PDMS) molds onto silicon wafers with nanofabricated microchannels. The devices were then peeled from the mold and 0.75 mm holes were punched for inlet and outlet tubing. A plasma etcher was used to bond the devices to glass slides and tubing was attached.

Sample Preparation

Polystyrene beads (780 nm in size) in phosphate buffer saline solution (PBS) were tracker dyed using Cell Tracker Green dye. Bead samples were pumped through single channel devices of varying size and curvature. This study focused on bead experiments through single-channel

devices with moderate curvature (200 μm at the inner wall and 400 μm at the outer wall) and rectangular cross-sections 50 μm by 200 μm.

Cultured cells (10-30 μm) at three protein concentrations (0, 3.5, and 7 g/dL) of bovine serum albumin (BSA) in PBS were tracker dyed using Cell Tracker Green dye. Cell samples were live during experimentation and used immediately. The device studied for cells had moderate curvature (200 μm at the inner wall and 400 μm at the outer wall) and three channels (top, middle, and bottom sections) of rectangular cross-sections 50 μm by 200 μm.

Flow Experiments

Before running samples, each device was prepped using a 1% (w/v) pluronic solution that could sit for a minimum of 10 minutes and run through the device using a Harvard Apparatus Syringe Pump to control the flow rate. After preparation, flow experiments were conducted by loading the samples into a syringe and running through the device using the same pump.

Image Capture

Images of the outlet portions of each device were recorded on a Nikon Eclipse LV100 Upright microscope (Figure 1). Flow was stabilized for a minimum of one minute before image capture. Images were analyzed using the Nikon Analysis Software. Lines were drawn across the device channel in the Nikon Analysis Software and the LUTs were exported.

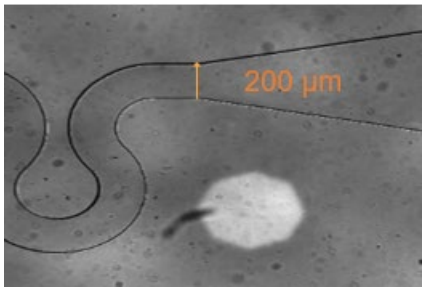

Figure 1. Sample channel outlet under microscope.

Fluorescence Characterization

Because the width dimension is significantly greater than the height dimension, analyses were done on particle focusing along the channel width. With relative fluorescence as a measurement of particle density, the LUT data was imported into MATLAB. The Find Peaks function was used to determine the peak height and full width at half-maximum, or FWHM (Figure 2). The peak height indicates the lateral focusing position of each streamline. The FWHM constitutes an average focusing width of each streamline.

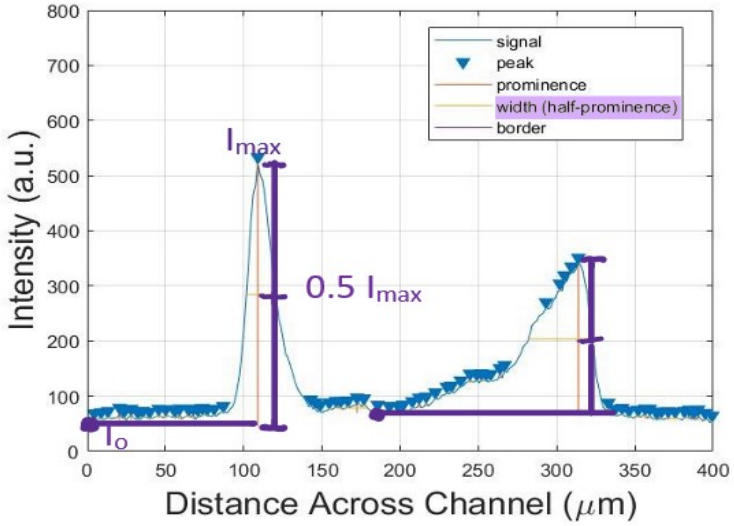

Figure 2. Find Peaks function output.
I_{max} refers to the peak intensity. The width was calculated at 0.5 I_{max}.

Results

Polystyrene Beads

The first goal of this study was to determine the best metric of inertial focusing. We did so by studying the effect of flow rate on the focusing of polystyrene beads, testing the devices at flow rates between 100 µL/min and 800 µL/min. Our results from polystyrene bead experiments confirmed previous studies on flow through curved microchannels.[2,3] Across the tested flow rates (for which streamlines are present), particles focus along both sides of the channel and streamlines were skewed towards the sides of the channel (Figure 3).

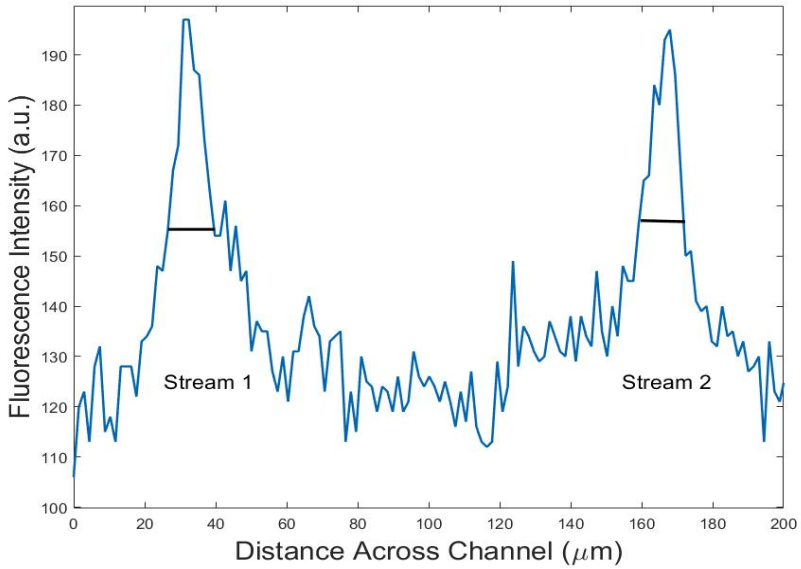

Figure 3. Fluorescence intensity across channel.

Additionally, particles focus along both sides of the channel at low flow rates and transition towards the center of the channel as the flow rate increases (Figure 4a). Streamline width is minimized at an intermediate flow rate of 350 µL/min, indicating inertial focusing is optimized under that condition (Figure 4b).

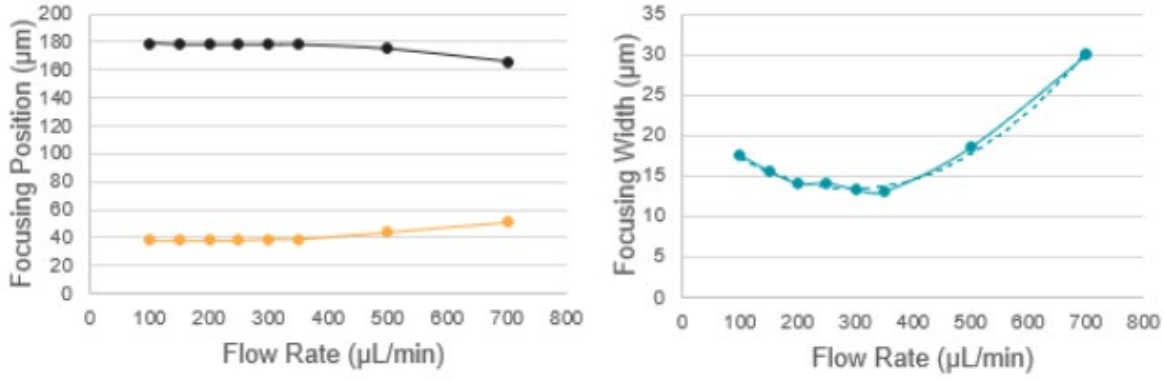

Figure 4. Lateral focusing position (a) and focusing width (b) with increasing flow rate.

From these results, we confirmed that FWHM analysis is an effective method to characterize the focusing width and therefore the average particle size flowing through a channel.

Cells

Following successful bead experiments, we used the same analysis methods to study the inertial focusing of cells. To better understand the effect of protein presence on cell focusing, cells were spiked into PBS (No BSA), 3.5 g/dL BSA, and 7 g/dL BSA solutions. These concentrations were selected because 7 g/dL is the typical protein concentration found in blood. All three solutions were tested at flow rates between 200 µL/min and 3600 µL/min in a device with three equivalent-sized channels. In all three channels of the device, particles quickly focused into streamlines at the channel centers.

The images on this page show the cell focusing patterns for the bottom section of the device in No BSA, 3.5 g/dL BSA, and 7 g/dL BSA conditions at select flow rates of 200, 666, and 1200 µL/min. The streams in the top section of the device behave very similarly. Across all three protein concentrations, one clear stream in the middle of the channel is present at 200 µL/min, the stream starts to split at 666 µL/min, and two streams form at 1200 µL/min. With increasing flowrate, focusing shifts from the outer wall to the inner wall. Nonetheless, cells are directed towards the center outlet across all flow rates.

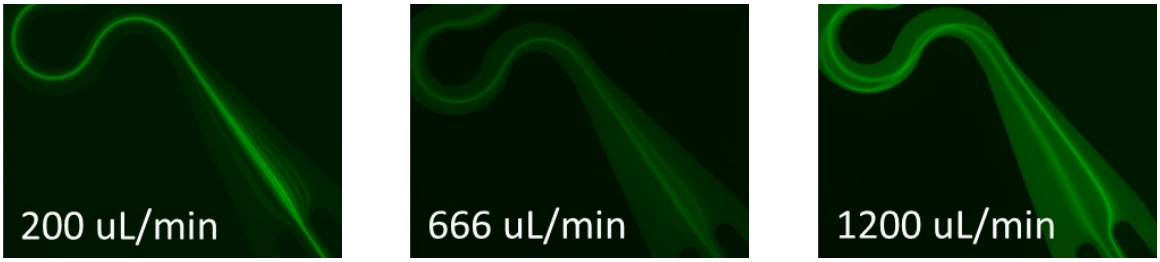

Figure 5a. Images of pre-fluoresced cells in PBS (No BSA) in the bottom channel of the device at specified flow rates.

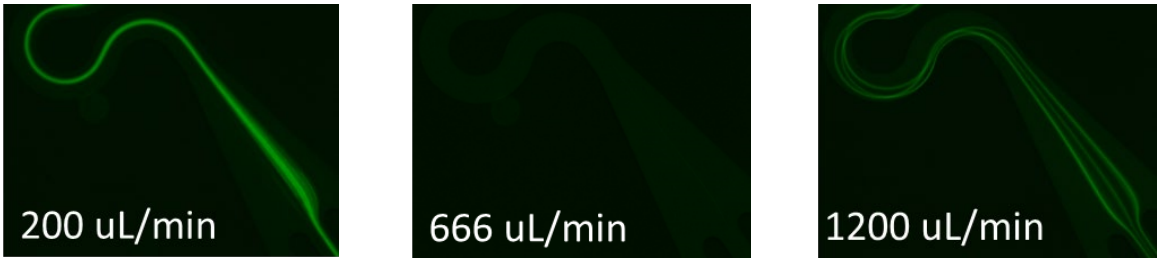

Figure 5b. Images of pre-fluoresced cells in 3.5 g/dL BSA in the bottom channel of the device at specified flow rates.

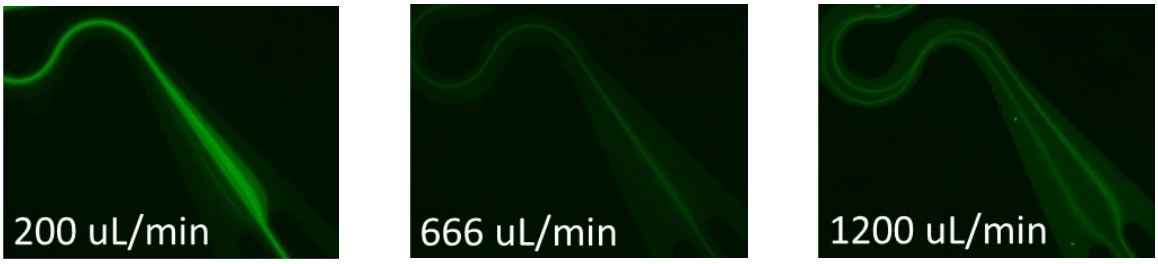

Figure 5c. Images of pre-fluoresced cells in 7 g/dL BSA in the bottom channel of the device at specified flow rates.

The graphs on this page present results for cell focusing in all three device sections, at select flow rates of 800, 2000, and 2400 µL/min. Fluorescence intensity values have been normalized to the maximum and minimum of each stream.

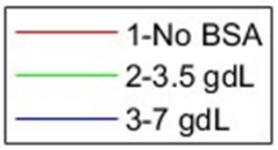

In the middle channel, focusing occurs at higher flows. Cells migrate to one streamline about 5-10 µm offset from the channel center (Figure 6a (ii) and (iii)).

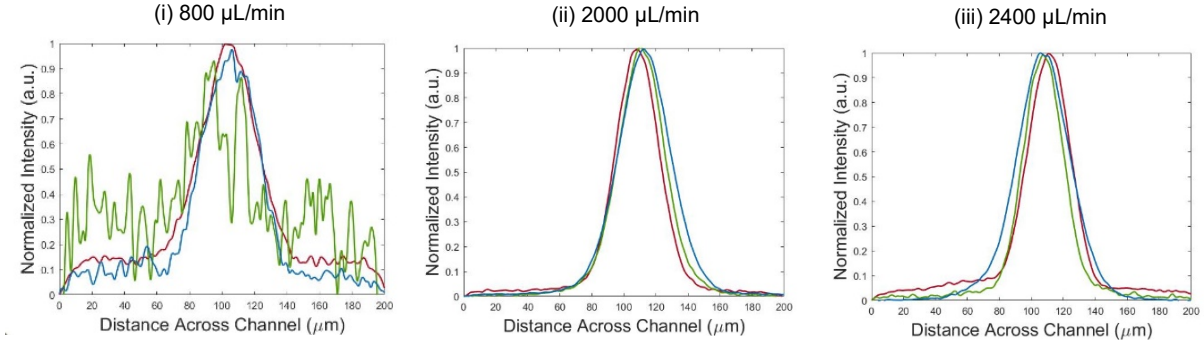

Figure 6a. Normalized fluorescent intensity graphs from the middle channel of the device.

In the bottom channel, focusing occurs at higher flows. Cells migrate to one streamline about 10-20 µm offset from the channel center (Figure 6b (i)).

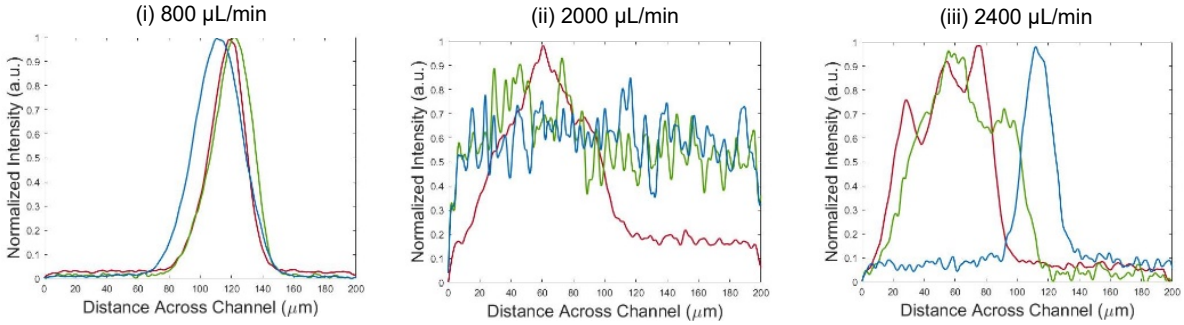

Figure 6b. Normalized fluorescent intensity graphs from the bottom channel of the device.

In the top channel, focusing also occurs at higher flows, with cells migrating to one streamline at nearly precisely the channel center (Figure 6c (i)).

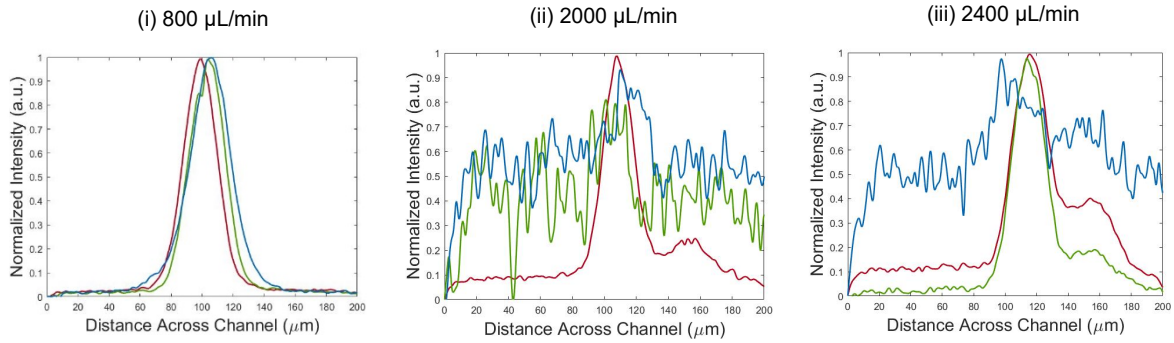

Figure 6c. Normalized fluorescent intensity graphs from the top channel of the device.

Using the Find Peaks function in MATLAB, smoothed fluorescence intensity curve characteristics were extracted, including peak intensity, location, and width at half-prominence. Width at half-prominence is a good indicator of how focused the cells are in a streamline. Each of the graphs in Figure 7 has datapoints for focusing widths averaged across the three protein concentrations plotted with respect to flow rate.

In the middle channel, the average focused streamline width is 37 μm (Figure 7a). As the stream width stayed between about 30-40 μm across flow rates, this indicates that cells of consistent size were directed towards the middle channel.

In the bottom and top channels, focusing occurred at lower flows. The average stream width is 31 μm and 30 μm at low flow rates for the bottom and top channels, respectively, and 21 μm and 18 μm at high flow rates for the bottom and top channels, respectively (Figure 7b and c).

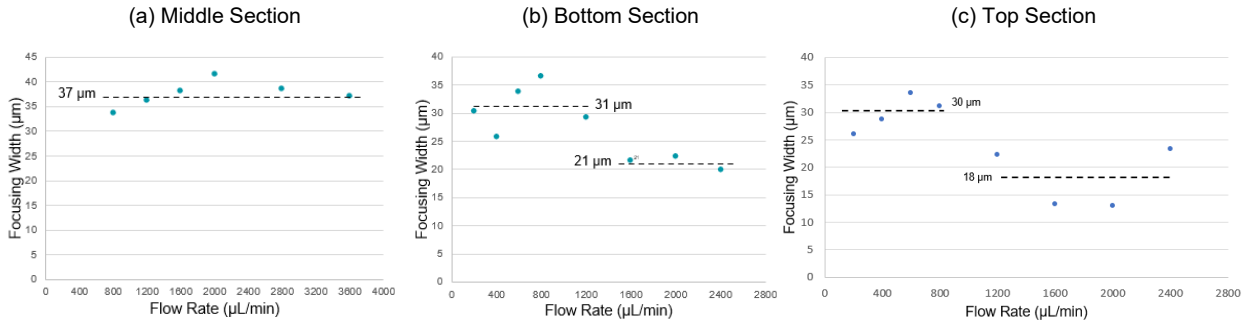

Figure 7. Focusing width across varying flow rate for each section of the device.

Discussion

Across all three protein concentrations, single peaks form in roughly the same position. Based on the peak widths at half-prominence, focusing becomes more distinct with increasing flow rate up to an intermediate flow rate. If flow rate continues to increase past this, focusing begins to be lost as the peak becomes wider.

For the middle channel, better focusing occurred at higher flow rates. This is because a greater percentage of cells flowed through the middle channel at higher flow rates, leading to greater inertial effects and thus better focusing. Stream width stayed between 30-40 μm across flow rates, indicating that cells of consistent size were directed towards the middle channel.

For the bottom and top channels, focusing was clearer at lower flow rates. This is because a greater percentage of cells flowed through the bottom and top channels at lower flow rates, leading to greater inertial effects and better focusing. At lower flow rates, the stream width was about 30 μm, while at higher flow rates, the stream width transitioned towards 20 μm, suggesting differences in separation of cells by size. As target cells were aimed to be collected from the outlets of the bottom and top channels, 800 μL/min was deemed the optimal flow rate. Much higher than this flow rate, focusing was worsened.

Conclusion

Inertial focusing is influenced by a variety of factors including velocity, density, viscosity, aspect ratio, and particle size. Although the cells tended to focus toward the center outlet of the device, the focusing patterns still differ depending on the media. While not discussed in this report, the study also compared cell focusing in buffer and whole blood, as buffer is a Newtonian fluid while whole blood is a non-Newtonian fluid. Although protein concentration did not significantly affect cell focusing in the results presented here, an increased protein concentration is speculated to lead to changes in particle properties particularly in non-Newtonian fluids. In the same size channel with the same curvature, bead experiments were run at lower flow rates and resulted in the formation of two streamlines, while cell experiments were expanded to higher flow rates and resulted in the formation of a single streamline. Further analysis is needed to compare the focusing of polystyrene beads to that of cells and distinguish changes in focusing patterns due to particle properties from those that are caused by differences in fluid properties.

The device presented in this report creates enriched streamlines using inertial focusing, performing the best at a moderate flow rate of 800 μL/min. The high percentage of cells that are focused in a label-free manner with this device shows opportunity for the detection of higher numbers of target cells in more patients. The use of this device will lead to better understanding of tumor migration and improved personalized medicine treatment by providing clinicians with additional phenotypic and genotypic information for their patients.

References

1. Di Carlo, D.; Edd, J., et al., *Physical Review Letters,* 2009, 102, 094503.
2. Martel, J.; Toner, M., *Annual Review of Biomedical Engineering*, 2014, 16, 371-396.
3. Ozbey, A.; Karimzadehkhouei, M., *Micro and Nano Engineering*, 2019, 2, 53-63.
4. Zhou, J.; Kulasinghe, A., *Microsystems & Nanoengineering*, 2019, 5, 8.